Modeling of stability of the condensing interface in a capillary pumped loop

Zheng-kai Tu [a], Mu Pan [a], Wei Liu [b,*], Zhi-chun Liu [b,*], Zhong-min Wan [c]

[a] State Key Laboratory of Advanced Technology for Materials Synthesis and Progressing, WUT, Wuhan 430070, China
[b] College of Energy and Power Engineering, Huazhong University of Science and Technology, Wuhan 430074, China
[c] Department of Physics, Hunan Institute of Science and Technology, Yueyang 414006, China

ARTICLE INFO

ABSTRACT

A mathematical model based on the Lucas–Washburn equation has been developed to address the relations of the capillary height, capillary radius and the heat flux in a capillary column and the equation is extended to a capillary loop for investigating the stability of the condensing interface with phase change by some simplifications in the paper. The stability of the condensing interface is studied by introducing a small disturbance into capillary height. The dynamics performances of the condensing interface under three different operating conditions are discussed in this paper. The results show that the condensing interface presents high instability under non-gravitational condition, while the stability can be enhanced in gravitational condition with a certain gravitational height, moreover, regular vibration can be formed on the condensing interface due to the periodic oscillation of the pressure in the system.

© 2011 Elsevier Ltd. All rights reserved.

1. Introduction

Capillary rise in porous media has been studied for many years. Basic understanding of the dynamics of capillary wetting can be dated back to the early 20th century [1,2]. The Lucas–Washburn equation is the basis for describing capillary phenomena. The dynamics of spontaneous capillary penetration into porous media are investigated by treating the media as parallel cylinders with the same radius. From then on, a series of theoretical and experimental studies have been done to present the practical applications of the Lucas–Washburn equation in porous medium [3–6]. Within the framework of the Lucas–Washburn equation, a force balance on a liquid body is considered, accounting for the forces due to capillarity, gravity, viscous drag and inertia. The main objective of present paper is to extend this equation to a capillary loop with phase change for investigating the stability of the condensing interface of a capillary loop with phase change by some simplifications.

Capillary loops (capillary pumped loop: CPL, loop heat pipe: LHP), which are derivatives of the heat pipe, are two-phase heat-transport devices which are capable of passively transporting heat over large distances with minimal temperature losses and have no moving parts for pumping the working fluid [7–15], so CPL/LHP is now the baseline design of thermal control for spacecrafts and electronics cooling. Liu et al. [16–24] have conducted widely investigation for CPL and LHP, including fluid flow and phase change heat transfer

in evaporator and condenser as well as performance test for system. Their investigation present that the performances of the system are related with the characteristics of evaporator and condenser as well as system configuration. Moreover, Liu et al. point that the CPL with a porous wick in the condenser can reduce even eliminate the pressure or temperature oscillations if the parameter of the condenser is reasonable. In the capillary loop, there are two interfaces, and they are evaporating interface and condensing interface, respectively, and there may be a third interface, that is interface in the reservoir (for CPL) or compensation chamber (for LHP). When heat load is applied to the evaporator, phase change may occur on the meniscus formed on the top of the wick. With the increasing of the heat load, the evaporating interface will gradually recede into the inner of the capillary wick, which will result in the dry-out of the evaporator. Therefore, the stability of the evaporating interface is involved in the operational status of the loop, researchers have paid more attentions to the evaporating interface [25–28], whereas the stability of the condensing interface is neglected. Pressure oscillations in CPL were firstly found by Ku and his co-workers [29,30], and temperature and pressure oscillations were also observed in visualization experiment by Kolos and Herold [31]. In particular, large amplitudes of the temperature oscillations were found in LHP [32,33,20], the closer to the condenser, the larger of the amplitude is [34]. As a result, it is very significant to investigate the dynamic motion of the condensing interface in the condenser.

2. Theoretical framework

To describe the rise of the liquid body in the capillary with phase change, Ramon and Oron [35] extended the Lucas–Washburn

* Corresponding authors. Tel.: +86 27 87542618; fax: +86 27 87540724.
E-mail addresses: tzklq@whut.edu.cn (Z.-k. Tu), panmu@whut.edu.cn (M. Pan), w_liu@hust.edu.cn (W. Liu), zcliu@hust.edu.cn (Z.-c. Liu), zhongminwan@sohu.com (Z.-m. Wan).

Nomenclature

σ	surface tension (N m^{-1})	u_0	steady state velocity (m s^{-1})
θ	contact angle (°)	t	time (s)
β	tilted angle (°)	p_v	vapor pressure (Pa)
R	capillary radius (m)	p_l	liquid pressure (Pa)
ρ	liquid density (kg m^{-3})	$\dot{m}$	interfacial mass flux (kg m^{-2} s^{-1})
ρ_v	vapor density (kg m^{-3})	Q	heat load (W)
g	gravitational acceleration (m s^{-2})	A	cross-section area (m^2)
s	capillary liquid length (m)	h_{fg}	latent heat (J kg^{-1})
H	equilibrium height/length (m)	$\varepsilon(t)$	small disturbance scale
s_0	condensing equilibrium length (m)	ΔH	gravitational height (m)
μ	liquid viscosity (kg m^{-1} s^{-1})	A_p	amplitude (m)
u	average axial velocity (m s^{-1})	ω	frequency (Hz)

equation in a vertical column, whereas for a tilted column, it can be described as (Fig. 1):

$$\frac{2\sigma\cos\theta}{R} - \rho gs\cos\beta - \Delta p - \frac{8\mu}{R^2}su = \frac{\rho d(su)}{dt} \tag{1}$$

where $\frac{2\sigma\cos\theta}{R}$ is the capillary force, $\rho gs\cos\beta$ is the gravity item, $\frac{8\mu}{R^2}su$ and $\frac{\rho d(su)}{dt}$ are the viscosity and inertia items, respectively. σ is the liquid–vapor surface tension, θ is the contact angle, R is the capillary radius, ρ is the liquid density, g is the gravitational acceleration, s is the length of the capillary liquid, β is the tilted angle with the vertical direction, μ is the viscosity of the liquid, u is the average axial velocity of the liquid, t is time, $\Delta p = p_v - p_l$, p_v and p_l are the static pressure on the top and bottom of the liquid column, respectively.

As for the interface, on one hand, the liquid is pumped back to the evaporator with a velocity of u by the capillary force, on the other hand, considering phase change occurs in the interface, liquid gain or loss will happens with the velocity of $\frac{\dot{m}}{\rho}$, hence, the kinematic boundary condition at the interface requires $u - \frac{ds}{dt} = \frac{\dot{m}}{\rho}$ [35], where $\dot{m}$ is the interfacial mass flux due to evaporation/condensation. Hence, Eq. (1) can be written as:

$$\frac{2\sigma\cos\theta}{R} - \rho gs\cos\beta - \Delta p - \frac{8\mu\dot{m}}{R^2\rho}s - \frac{8\mu}{R^2}s\frac{ds}{st} - \frac{\dot{m}^2}{\rho_v}$$
$$= \rho\frac{d}{dt}\left(s\frac{\dot{m}}{\rho} + s\frac{ds}{dt}\right) \tag{2}$$
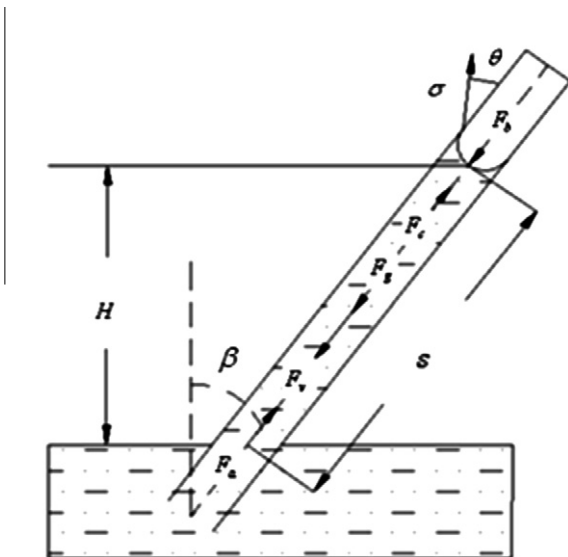

Fig. 1. The force balance in the capillary liquid column.

where $\frac{\dot{m}^2}{\rho_v}$ is named as vapor recoil, and it can also be expressed as $\frac{Q^2}{A^2 h_{fg}^2 \rho_v}$, where Q is the heat load added to the system, A is the cross-section area of the column, h_{fg} is the latent heat of vaporization, and ρ_v is the vapor density. Under steady state, Eq. (2) reduces to

$$\frac{2\sigma\cos\theta}{R} - \rho gs\cos\beta - \Delta p - \frac{\dot{m}^2}{\rho_v} - \frac{8\mu\dot{m}}{R^2\rho}s = 0 \tag{3}$$

Eq. (3) shows that the capillary force will balance not only the pressure difference across the interface and the vapor recoil but also the viscosity and gravity of the liquid in the steady state.

3. Results and discussion

The geometrical parameters in Fig. 1 are as follows: the equilibrium length of the liquid column is $s_0 = 0.3$ m, and the inner radius R of the condensing pipe is 1×10^{-3} m. The working fluid is methanol, and its properties are given in Table 1 [36].

3.1. Stability under non-gravitational condition

Eq. (2) can be rewritten as follow under non-gravitational condition:

$$\frac{2\sigma\cos\theta}{R} - \Delta p - \frac{\dot{m}^2}{\rho_v} - \frac{8\mu\dot{m}}{R^2\rho}s - \frac{8\mu}{R^2}s\frac{ds}{st} = \rho\frac{d}{dt}\left(s\frac{\dot{m}}{\rho} + s\frac{ds}{dt}\right) \tag{4}$$

Based on Ramon and Oron's model [35], considering the stability of the steady equilibrium length s_0 of the liquid column by introducing a small disturbance in the form as follow:

$$s = s_0 \pm \varepsilon(t)s_0 \quad (0 < \varepsilon \ll 1) \tag{5}$$

Because $\varepsilon(t) \ll 1$, substituting Eq. (5) into Eq. (4) and linearizing the latter with respect to $\varepsilon(t)$, it gets

$$\varepsilon''(t) + a\varepsilon'(t) + b\varepsilon(t) = 0 \tag{6}$$

where $a = \frac{u_0}{s_0} + \frac{8\mu}{\rho R^2}$ and $b = \frac{u_0}{s_0}\frac{8\mu}{\rho R^2}$, u_0 is the steady state velocity, it is negative because it is opposite with the stipulation direction in the condensing state, while it is positive when evaporating occurs. As a consequence, b is also negative in Eq. (6). Generally, $|\frac{u_0}{s_0}|$ is far less than $|\frac{8\mu}{\rho R^2}|$ in the practical applications, so a is positive. Compared with

Table 1
Physical properties of methanol at 37 °C.

ρ_l (kg m^{-3})	ρ_v (kg m^{-3})	μ (kg s^{-1} m^{-1})	σ (N m^{-1})	h_{fg} (J kg^{-1})
7.78×10^2	0.48	4.8×10^{-4}	2.11×10^{-2}	1.14×10^6

the evaporating state, the differences of the parameters in Eq. (6) will result in a distinct behavior of the interface in the condenser.

Fig. 2 shows the evolutions of the positive and negative small disturbances in different heat loads. As can be seen, both the positive and the negative small disturbances are enlarged in the condensing interface, and the heat load plays an obvious effect on the dynamics motion of the condensing interface. When the heat load is 5 W, the disturbances are enlarged by 10 times after about 1000 s, it can reduce to about 250 s at 20 W. What is more, for a negative small disturbance, the condensing interface has strong tendency to move towards the liquid side, however, the liquid is incompressible, therefore, strong instability is forming in the condensing interface. For a positive small disturbance, the interface tends to move towards the vapor while the vapor rushes at the interface in a high speed. As a consequence, the collision in the interface will also result in a strong instability, and the condensing interface has a stronger instability than the evaporating interface.

3.2. Stability in gravitational condition

In gravitational condition, b in Eq. (6) is written as $b = \frac{g}{s_0}\cos\beta + \frac{u_0}{s_0}\frac{8\mu}{\rho R^2}$. Here $\cos\beta = \frac{\Delta H}{s_0}$ and ΔH is the gravitational height of the capillary liquid. s_0 and ΔH are shown in Fig. 3.

Fig. 4 shows the decline evolutions of the positive and negative disturbance in different gravitational heights. As can be seen, the

evolutions of the positive and negative disturbance are nearly symmetrical. The small disturbances are not enlarged, on the contrary, both of them decline towards the equilibrium position. As a consequence, the stability of the interface is enhanced in gravitational condition. It can also be seen that the decline time to the quasi-equilibrium position is decrease with the increasing of the gravitational height. According to mathematical analysis, Eq. (6) will be a monotonic decline curve as long as a and b are both positive. Hence, to enhance the stability of the interface, it requires that

$$\cos\beta > \frac{|u_0|}{g}\frac{8\mu}{\rho R^2} \quad \text{or} \quad \frac{\Delta H}{s_0} > \frac{|u_0|}{g}\frac{8\mu}{\rho R^2} \tag{7}$$

Fig. 5 presents the time evolution of the relative velocity $\varepsilon'(t)$ in the gravitational condition. Considering the comparability of the velocities of the interface at the different condensing length, we take the evolution of the relative velocity curve at the condensing length of 0.3 m for illustration. Considering a and b are both positive, the discriminant $\Omega = a^2 - 4b > 0$ and a is larger than b, Eq. (6) is a over-damped equation with high damp in this situation. For a given small disturbance, it will decline to the quasi-equilibrium position rapidly, and the stability of the interface will be enhanced greatly in this case.

The time evolutions of the small disturbance under the different heat loads in gravitational condition are shown in Fig. 6. For the same disturbance, it will take a longer time to decline to the quasi-equilibrium position with the increasing of the heat load, which indicates that the instability of the interface is aggrandizing under the high heat load. On the other hand, the mechanisms of the instability under high heat load are quite different under non-gravitational and gravitational conditions, that is, disturbance is enlarged under non-gravitational condition whereas it is declining in gravitational condition with a certain gravitational height, and the interface presents better stability in gravitational condition.

3.3. Stability in practical operation

Pressure oscillations are found in the system during the normal operation [29–31], therefore, Eq. (4) under non-gravitational condition can be written as:

$$\frac{2\sigma\cos\theta}{R} - \Delta p - A_p \sin(\omega t) - \frac{\dot{m}^2}{\rho_v} - \frac{8\mu\dot{m}}{R^2\rho}s - \frac{8\mu}{R^2}s\frac{ds}{st}$$
$$= \rho\frac{d}{dt}\left(s\frac{\dot{m}}{\rho} + s\frac{ds}{dt}\right) \tag{8}$$

where A_p and ω are the amplitude and frequency of the pressure, respectively, and Eq. (6) will be written as:

$$\varepsilon''(t) + a\varepsilon'(t) + b\varepsilon(t) = \frac{A_p}{\rho s_0^2}\sin(\omega t) = f\sin(\omega t) \tag{9}$$

The evolutions of the positive and negative disturbances in the normal operation under non-gravitational condition are present in Fig. 7. The evolutions of the disturbances are both wavy. What's more, unlike Fig. 2, both the positive and negative curves evolve towards the same side in the end due to the oscillations of the pressure in Fig. 7. As a consequence, the effect of the vapor recoil is overwhelmed by the pressure oscillations, and the later becomes the dominant mechanism influencing the dynamics motion of the condensing interface.

Fig. 8 shows the evolutions of the positive and negative disturbances in the normal operation with a certain gravitational height. The positive and negative curves are overlapping and waving with a certain amplitude after several seconds. The frequency of the evolution is the same as the pressure oscillations. In this situation, Eq. (9) can be written as:
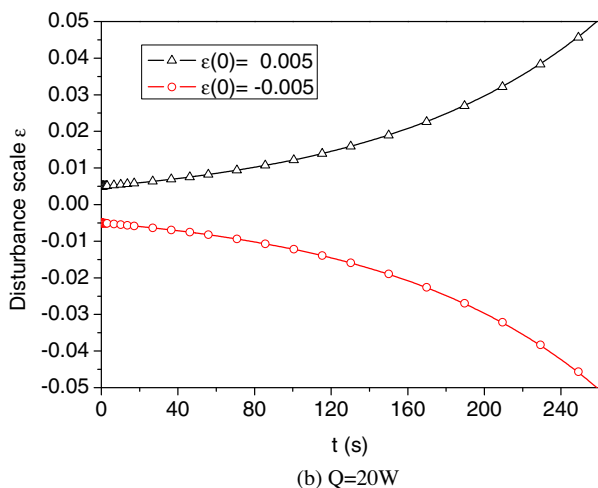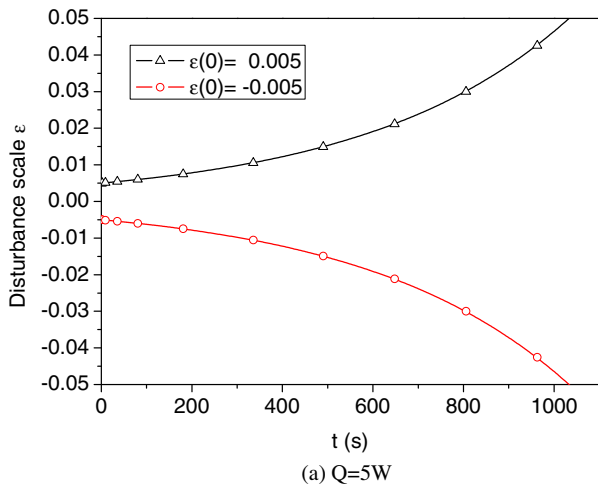

Fig. 2. The evolutions of the small disturbances in different heat fluxes ($s_0 = 0.3$ m, $R = 1 \times 10^{-3}$ m). (a) Q = 5 W and (b) Q = 20 W.
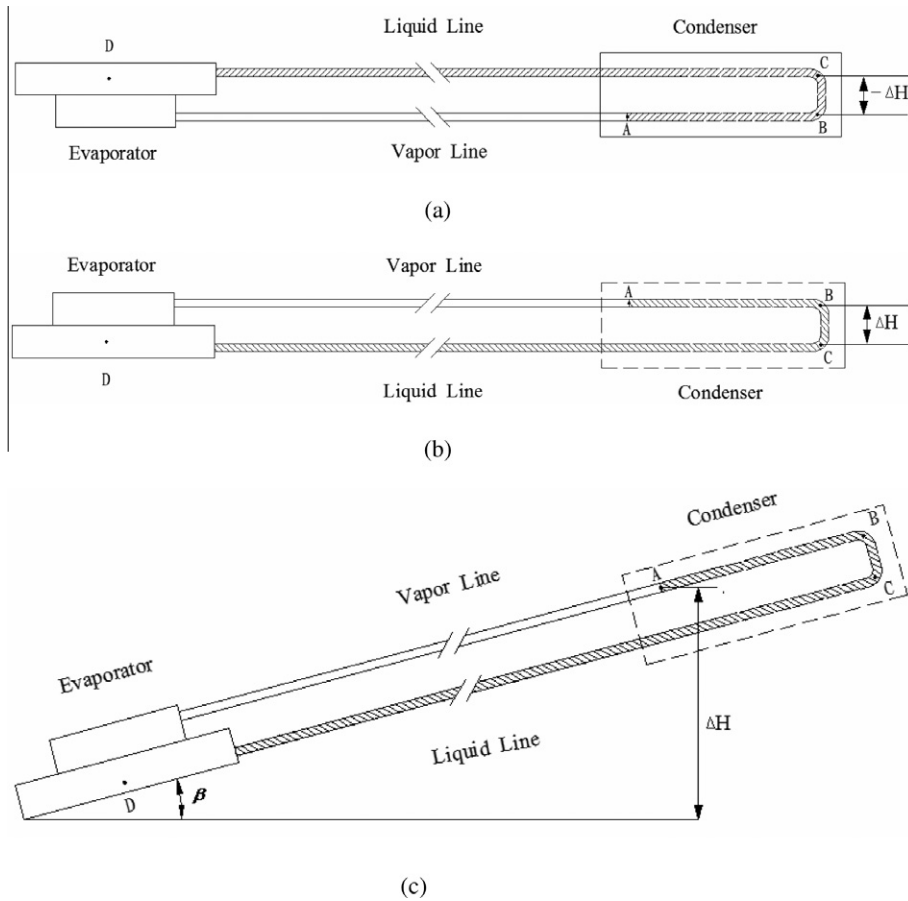
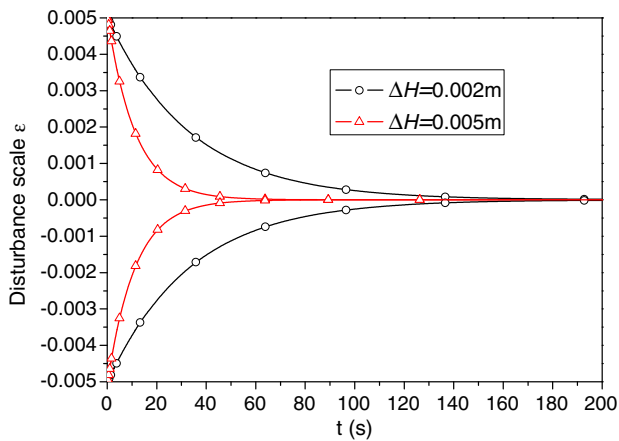**Fig. 3.** The relations of s_0 and ΔH ($s_0 = AB + BC + CD$).

Fig. 4. The evolution of the small disturbances in different gravitational heights ($s_0 = 0.3$ m, $R = 1 \times 10^{-3}$ m, $Q = 20$ W).
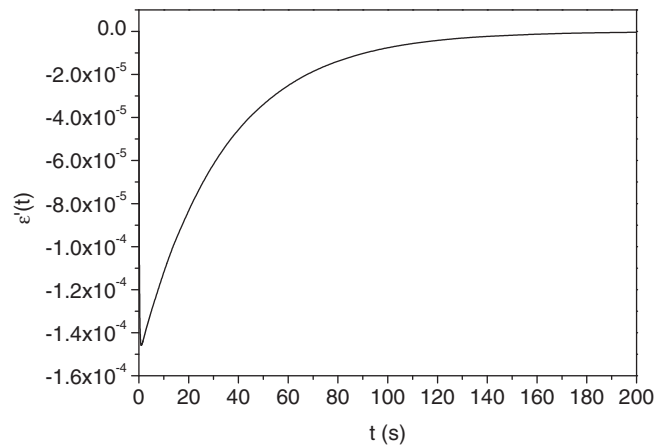

Fig. 5. The evolution of the relative velocity $\varepsilon'(t)$ with time t in gravitational condition ($Q = 20$ W, $s_0 = 0.3$ m, $\Delta H = 0.002$ m).

$$\varepsilon''(t) + a\varepsilon'(t) + b\varepsilon(t) = f\sin(\omega t) \tag{10}$$

When the discriminant $\Omega = a^2 - 4b \geqslant 0$, the analytical solution of Eq. (10) is given as:

$$\varepsilon(t) = c_1 e^{-k_1 t} + c_2 e^{-k_2 t} + \frac{f}{\sqrt{(\omega^2 - b)^2 + a^2 \omega^2}}\sin(\omega t + \varphi)$$

When the discriminant $\Omega = a^2 - 4b < 0$, the analytical solution of Eq. (10) can be gained:

$$\varepsilon(t) = c_3 e^{-\frac{a}{2}t} \cdot \cos(\omega_1 t + \varphi_1) + \frac{f}{\sqrt{(\omega^2 - b)^2 + a^2 \omega^2}}\sin(\omega t + \varphi)$$

where k_1 and k_2 are both positive in the solution, c_1, c_2, c_3, ω_1 and φ_1 are coefficients corresponding to the initialization conditions, $\tan\varphi = \frac{\omega^2 - b}{a\omega}$, hence, whether Ω is positive, negative or zero, after a long time, a steady wave is forming in the condensing interface, and it can be expressed as:
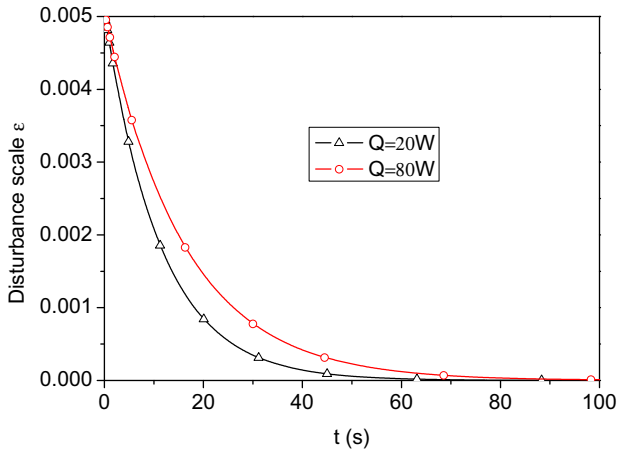
Fig. 6. The evolutions of the small disturbances in different heat loads in gravitational condition ($s_0 = 0.3$ m, $\Delta H = 0.005$ m).
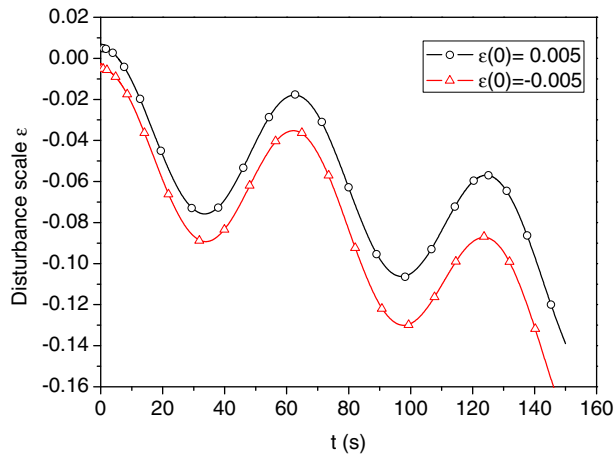

Fig. 7. The evolutions of the small disturbances with pressure oscillations in the system in non-gravitational condition ($Q = 20$ W, $s_0 = 0.3$ m, $f = 0.02$, $\omega = 0.1$ Hz).
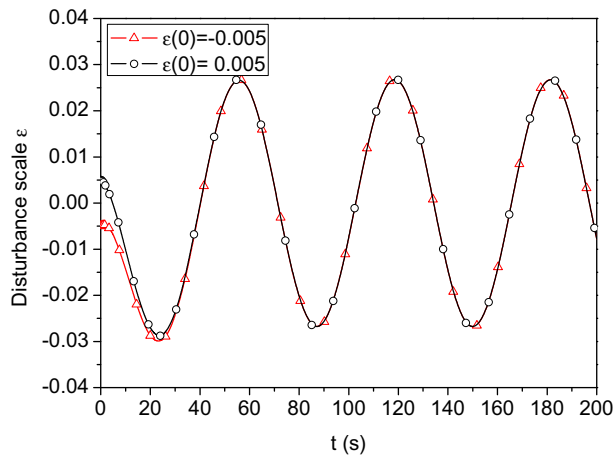

Fig. 8. The evolutions of the positive and negative disturbances in the normal operation ($Q = 20$ W, $s_0 = 0.3$ m, $\Delta H = 0.005$ m, $f = 0.02$, $\omega = 0.1$ Hz).

$$\varepsilon(t) = \frac{f}{\sqrt{(\omega^2 - b)^2 + a^2\omega^2}} \sin(\omega t + \varphi) \tag{11}$$

Eq. (11) shows that for an arbitrary initialization of the small disturbance, a steady sinusoidal motion of the interface can be formed due to the fluctuation of the pressure, and it has the same frequency with the pressure oscillations. Furthermore, the amplitude is a function of the heat load, radius and length of the condensing pipe, the physical properties of the working fluid. For a steady state corresponding to a certain heat load, the amplitude of the fluctuation can be written as:

$$\varepsilon(t)_{max} = \frac{f}{\sqrt{\omega^4 + (a^2 - 2b)\omega^2 + b^2}} \tag{12}$$

When $a^2 - 4b \geqslant 0$, the discriminant of Eq. (12) $\Omega \geqslant 0$, and the amplitude decreases with the increasing of the heat load.

When $a^2 - 4b < 0$, the discriminant of Eq. (12) $\Omega < 0$, if $a^2 - 2b \geqslant 0$, the same evolution tendency of the amplitude can be got as $\Omega \geqslant 0$, while $a^2 - 2b < 0$, the amplitude will turn to a parabola evolution.

Generally, the capillary loops operate under the micro-gravity condition with $\Omega \geqslant 0$, for a given heat load, the amplitude increases with the decrease of the frequency of the pressure oscillation (seen in Fig. 9), and for a steady pressure oscillation, the amplitude will increase with the increasing of heat load (seen in Fig. 10).

Based on the above analyses, we can know that the pressure oscillations play an important role on the dynamic motion of the interface. The dynamics motion of the condensing interface is easier disturbed by the pressure oscillations than that of the evaporator, because the dimensions of the capillary pores is far less than the wavelength of the pressure oscillations in the evaporator, and the transmission of the pressure oscillations will be reflected by the capillary structure. Pendyala et al. [37] pointed out the average Reynolds numbers (Re_{mean}) of the flow can be enhanced due to the oscillations of the pressure. According to Eq. (11) and the expression of the absolute velocity u of the liquid in the condensing pipe in the theoretical framework, we can know that

$$u = \frac{f\omega s_0}{\sqrt{(\omega^2 - b)^2 + a^2\omega^2}} \cos(\omega t + \varphi) + u_0 \tag{13}$$

where u_0 is arose from the phase change, while the first term of Eq. (13) in the right hand is coming from the pressure oscillations, and the positive or negative average value of the first term in a half period can be got as $u_{av} = \frac{f\omega s_0}{\pi\sqrt{(\omega^2-b)^2+a^2\omega^2}}$ by integral. Fig. 11 shows $\frac{u_{av}}{u_0}$ in different heat loads, as can be seen, the ratio decreases with the increasing of the heat load, and the ratio is larger than 1 even at
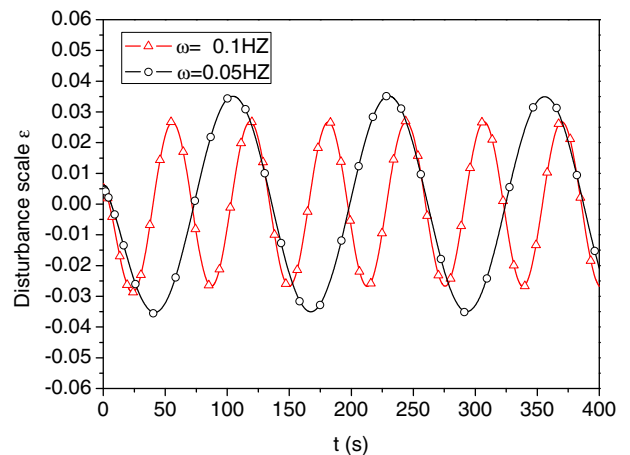

Fig. 9. The evolutions of the small disturbances in different frequencies in practical operation ($Q = 20$ W, $s_0 = 0.3$ m, $\Delta H = 0.005$ m, $f = 0.02$).
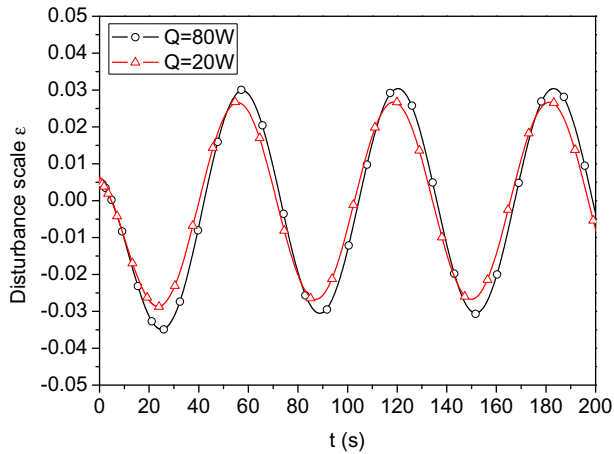
Fig. 10. The evolutions of the small disturbances in different heat loads in practical operation (s_0 = 0.3 m, ΔH = 0.005 m, f = 0.02, ω = 0.1 Hz).
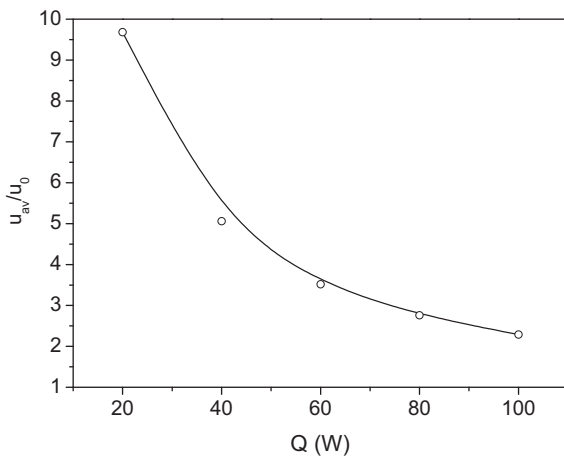

Fig. 11. $\frac{u_{av}}{u_0}$ in different heat loads (s_0 = 0.3 m, ΔH = 0.005 m, f = 2, ω = 0.1 Hz).

the heat load of 100 W, so the heat transfer performance can be enhanced in the system. Staples [38] presented an attractive flow in a sinusoidal capillary, and we can use a sinusoidal tube as the flowing path of the vapor to gain steady pressure oscillations, and large amplitude. For example, f = 2 in Fig. 11, in this case, heat transfer in the condensing line can be enhanced by this positive means, and it can be extended to the situation in the capillary or micro structure for high heat flux removal.

4. Conclusions

The stability of the condensing interface in a capillary loop is well demonstrated based on the extended Lucas–Washburn equation with phase change, and the following conclusions can be formulated as:

(1) The interface shows strong instability under non-gravitational condition, and the instability increases with the increasing of the heat load in the system.
(2) With a certain gravitational, the motion of the interface will turn into an over-damped evolution, and the stability of the interface can be greatly enhanced.
(3) With the existence of the pressure oscillations in the loop, the motion of the interface will show a wavy evolution. A steady sinusoidal motion of the interface can be formed in the gravitational condition, the fluctuation of the interface

has the same frequency with the pressure oscillations, and the amplitude is a function of the heat load, radius and length of the condensing pipe, the physical properties of the working fluid.

(4) Heat transfer performance of the system in the liquid transport line can be enhance due to the fluctuations of the pressure, and a sinusoidal tube can be used as the vapor flowing path to produce a steady pressure oscillations in the loop, as a consequence, this positive heat transfer means can be extended to the situation in the capillary or micro structure for large heat flux removal.

References

[1] R. Lucas, Ueber das zeitgesetz des kapillaren aufstiegs von flussigkeiten, Kolloidn Zh. 23 (1918) 15–22.
[2] E.W. Washburn, The dynamics of capillary flow, Phys. Rev. 17 (3) (1921) 273–283.
[3] D.I. Dimitrov, A. Milchev, K. Binder, Capillary rise in nanopores: molecular dynamics evidence for the Lucas–Washburn equation, Phys. Rev. Lett. 99 (5) (2007) 054501.
[4] A. Marmur, in: M.E. Stirred, G.I. Lobe (Eds.), Modern Approach to Wettability: Theory and Application, Plenum Press, New York, 1992.
[5] S. Ahadian, S. Moradian, F. Sharif, et al., Application of artificial neural network (ANN) in order to predict the surface free energy of powders using the capillary rise method, Colloids Surf. A 302 (2007) 280–285.
[6] M. Karoglou, A. Moropoulou, A. Giakoumaki, et al., Capillary rise kinetics of some building materials, J. Colloid Interface Sci. 284 (2005) 260–264.
[7] Y.F. Maidanik, Loop heat pipe, Appl. Therm. Eng. 25 (2005) 635–657.
[8] V.G. Pastukhov, Y.F. Maydanik, C.V. Vershinin, M.A. Korukov, Miniature loop heat pipes for electronic cooling, Appl. Therm. Eng. (23) (2003) 1125–1135.
[9] I. Muraoka, F.M. Ramos, V.V. Vlassov, Experimental and theoretical investigation of a capillary pumped loop with a porous element in the condenser, Int. Commun. Heat Mass Transfer 25 (8) (1998) 1085–1094.
[10] P.C. Chen, W.K. Lin, The application of capillary pumped loop for cooling of electronic components, Appl. Therm. Eng. 21 (11) (2001) 1739–1754.
[11] A.S. Demidov, E.S. Yatsenko, Investigation of heat and mass transfer in the evaporation zone of a heat pipe operating by the 'inverted meniscus' principle, Int. J. Heat Mass Transfer 37 (1994) 2155–2163.
[12] H. Teng, P. Cheng, T.S. Zhao, Instability of condensate film and capillary blocking in small-diameter thermosyphon condensers, Int. J. Heat Mass Transfer 42 (1999) 3071–3083.
[13] D.R. Chalmers, J.J. Pustay, C.B. Moy, et al., Application of capillary pumped loop heat transport systems to large spacecraft, AIAA Paper 86-1295, 1986.
[14] D. Khrustalev, A. Faghri, Heat transfer in the inverted meniscus type evaporator at high heat fluxes, Int. J. Heat Mass Transfer 38 (1995) 3091–3101.
[15] T.S. Zhao, Q. Liao, On capillary-driven flow and phase-change heat transfer in a porous structure heated by a finned surface: measurements and modeling, Int. J. Heat Mass Transfer 43 (2000) 1141–1155.
[16] Z.C. Liu, W. Liu, J.G. Yang, Experimental investigation of new flat-plate-type capillary pumped loop, J. Thermophys. Heat Transfer 22 (1) (2008) 98–104.
[17] Z.C. Liu, W. Liu, J.G. Yang, Design and experimental research of a flat-plate type CPL with a porous wick in the condenser, J. Enhanced Heat Transfer 16 (2) (2009) 161–170.
[18] Z.C. Liu, W. Liu, A. Nakayama, Flow and heat transfer analysis in porous wick of CPL evaporator based on field synergy principle, Heat Mass Transfer 43 (2007) 1273–1281.
[19] Z.C. Liu, D.X. Gai, H. Li, et al., Investigation of impact of different working fluids on the operational characteristics of miniature LHP with flat evaporator, Appl. Therm. Eng. 31 (2011) 3387–3392.
[20] D.X. Gai, W. Liu, Z.C. Liu, Temperature oscillation of mLHP with flat evaporator, Heat Transfer Res. 40 (4) (2009) 321–332.
[21] D.X. Gai, Z.C. Liu, W. Liu, J.G. Yang, Operational characteristics of miniature loop heat pipe with flat evaporator, Heat Mass Transfer 46 (2009) 267–275.
[22] Z.M. Wan, W. Liu, Z.K. Tu, A. Nakayama, Conjugate numerical analysis of flow and heat transfer with phase change in a miniature flat plate CPL evaporator, Int. J. Heat Mass Transfer 52 (2009) 422–430.
[23] Z.K. Tu, Z.C. Liu, C. Liu, D.X. Gai, Z.M. Wan, W. Liu, Heat and mass transfer in a flat disc-shaped evaporator of a miniature loop heat pipe, Proc. IMechE J. Aerosp. Eng. 223 (2009) 609–618.
[24] W. Liu, Z.C. Liu, K. Yang, Z.K. Tu, Phase change driving mechanism and modeling for heat pipe with porous wick, Chin. Sci. Bull. 54 (21) (2009) 4000–4004.

[25] M.A. Hanlon, H.B. Ma, Evaporation heat transfer in sintered porous media, J. Heat Transfer 125 (4) (2003) 644–652.

[26] L. Chen, G.P. Peterson, Y.X. Wang, Evaporation/boiling in thin capillary wicks(I)–wick thickness effects, J. Heat Transfer 128 (12) (2006) 1312–1319.

[27] H. Wang, S.V. Garimella, J.Y. Murthy, Characteristics of an evaporating thin film in a microchannel, Int. J. Heat Mass Transfer 50 (2007) 3933–3942.

[28] J.T. Zhang, B.X. Wang, Effect of capillarity at liquid–vapor interface on phase change without surfactant, Int. J. Heat Mass Transfer 45 (2002) 2689–2694.

[29] J. Ku, T.D. Swanson, et al., Flow visualization within a capillary evaporator, SAE Paper No. 932236, in: Proceedings of the 23rd International Conference on Environmental Systems, July 12–15, 1993.

[30] T. O'Connell, T. Hoang, J. Ku, Investigation of power turn down transients in CAPL-1 flight experiment, AIAA Paper No. 952067, in: Proceedings of the 30th AIAA Thermophysics Conference, June 19–22, 1995, San Diego, CA, pp. 1–7.

[31] K.R. Kolos, K.E. Herold, Low temperature and fluid oscillations in capillary pumped loops, in: Proceedings of the National Heat Transfer Conference, Baltimore, Maryland, August 10–12, 1997, pp. 1–8.

[32] S.V. Vershinin, Y.F. Maydanik, Investigation of pulsations of the operating temperature in a miniature loop heat pipe, Int. J. Heat Mass Transfer 50 (2007) 5232–5240.

[33] R. Singh, A. Akbarzadeh, A. Mochizuki, Operational characteristics of a miniature loop heat pipe with flat evaporator, Int. J. Therm. Sci. 47 (11) (2008) 1504–1515.

[34] Y.M. Chen, M. Groll, et al., Steady-state and transient performance of a miniature loop heat pipe, Int. J. Therm. Sci. 45 (2006) 1084–1090.

[35] G. Ramon, A. Oron, Capillary rise of a meniscus with phase change, J. Colloid Interface Sci. 327 (2008) 145–151.

[36] D.R. Lide (Ed.), CRC Handbook of Chemistry and Physics, 87th ed., Taylor and Francis, Boca Raton, 2007, Available from: <http://www.hbcpnetbase.com>.

[37] R. Pendyala, S. Jayanti, A.R. Balakrishnan, Flow and pressure drop fluctuations in a vertical tube subject to low frequency oscillations, Nucl. Eng. Des. 238 (2008) 178–187.

[38] T.L. Staples, D.G. Shaffer, Wicking flow in irregular capillaries, Colloids Surf. A 204 (2002) 239–250.